Environmental Science & Technology

Article

pubs.acs.org/est

High Density Ozone Monitoring Using Gas Sensitive Semi-Conductor Sensors in the Lower Fraser Valley, British Columbia

Mark Bart,[†] David E Williams,[‡] Bruce Ainslie,[§] Ian McKendry,*[,∥] Jennifer Salmond,[⊥] Stuart K. Grange,[‡] Maryam Alavi-Shoshtari,[#] Douw Steyn,[▽] and Geoff S. Henshaw[◇]

[†]Air Quality Ltd., P.O. Box 24 443, Auckland 1345, New Zealand

[‡]MacDiarmid Institute for Advanced Materials and Nanotechnology, School of Chemical Sciences, The University of Auckland, Science Centre, Building 301, 23 Symonds Street, Auckland 1142, New Zealand

[§]Environment Canada, 401 Burrard Street, Vancouver, British Columbia V6C 3S5, Canada

[∥]Department of Geography, The University of British Columbia, 1984 West Mall, Vancouver, British Columbia V6T 1Z2, Canada

[⊥]School of Environment, The University of Auckland, Private Bag 92019, Auckland 1142, New Zealand

[#]Department of Mathematics, The University of Auckland, 38 Princes Street, Auckland 1010, New Zealand

[▽]Earth, Ocean and Atmospheric Science, The University of British Columbia, Room 2020, Earth Sciences Building, 2207 Main Mall, Vancouver, British Columbia V6T 1Z4, Canada

[◇]Aeroqual Ltd., 109 Valley Road, Mount Eden, Auckland 1024, New Zealand

Supporting Information

ABSTRACT: A cost-efficient technology for accurate surface ozone monitoring using gas-sensitive semiconducting oxide (GSS) technology, solar power, and automated cell-phone communications was deployed and validated in a 50 sensor test-bed in the Lower Fraser Valley of British Columbia, over 3 months from May–September 2012. Before field deployment, the entire set of instruments was colocated with reference instruments for at least 48 h, comparing hourly averaged data. The standard error of estimate over a typical range 0–50 ppb for the set was 3 ± 2 ppb. Long-term accuracy was assessed over several months by colocation of a subset of ten instruments each at a different reference site. The differences (GSS-reference) of hourly average ozone concentration were normally distributed with mean −1 ppb and standard deviation 6 ppb (6000 measurement pairs). Instrument failures in the field were detected using network correlations and consistency checks on the raw sensor resistance data. Comparisons with modeled spatial O_3 fields demonstrate the enhanced monitoring capability of a network that was a hybrid of low-cost and reference instruments, in which GSS sensors are used both to increase station density within a network as well as to extend monitoring into remote areas. This ambitious deployment exposed a number of challenges and lessons, including the logistical effort required to deploy and maintain sites over a summer period, and deficiencies in cell phone communications and battery life. Instrument failures at remote sites suggested that redundancy should be built into the network (especially at critical sites) as well as the possible addition of a "sleep-mode" for GSS monitors. At the network design phase, a more objective approach to optimize interstation distances, and the "information" content of the network is recommended. This study has demonstrated the utility and affordability of the GSS technology for a variety of applications, and the effectiveness of this technology as a means substantially and economically to extend the coverage of an air quality monitoring network. Low-cost, neighborhood-scale networks that produce reliable data can be envisaged.

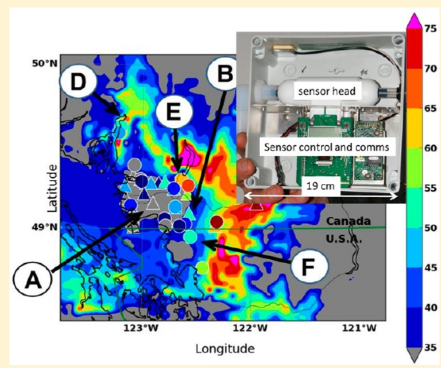

INTRODUCTION

Ozone (O_3) monitoring is a critical component of air quality management in urban airsheds. To date, monitoring strategies have traditionally involved expensive fixed site monitors deployed in purpose built and secure facilities. Often, such networks are sparse and not well suited to particular applications such as population exposure studies or specific research applications (e.g., mapping the fine scale distribution of O_3 concentrations across broad and sometimes complex regions). The advent of new miniaturized technologies, solar panels, and cell phone networks has created the opportunity to develop low cost flexible networks at high resolution, potentially on the scale of thousands of devices. These include a low cost cell-phone based system for monitoring of black carbon[1] and similar low cost wireless initiatives in Lahore,

Received: December 4, 2013
Revised: February 7, 2014
Accepted: February 28, 2014
Published: February 28, 2014

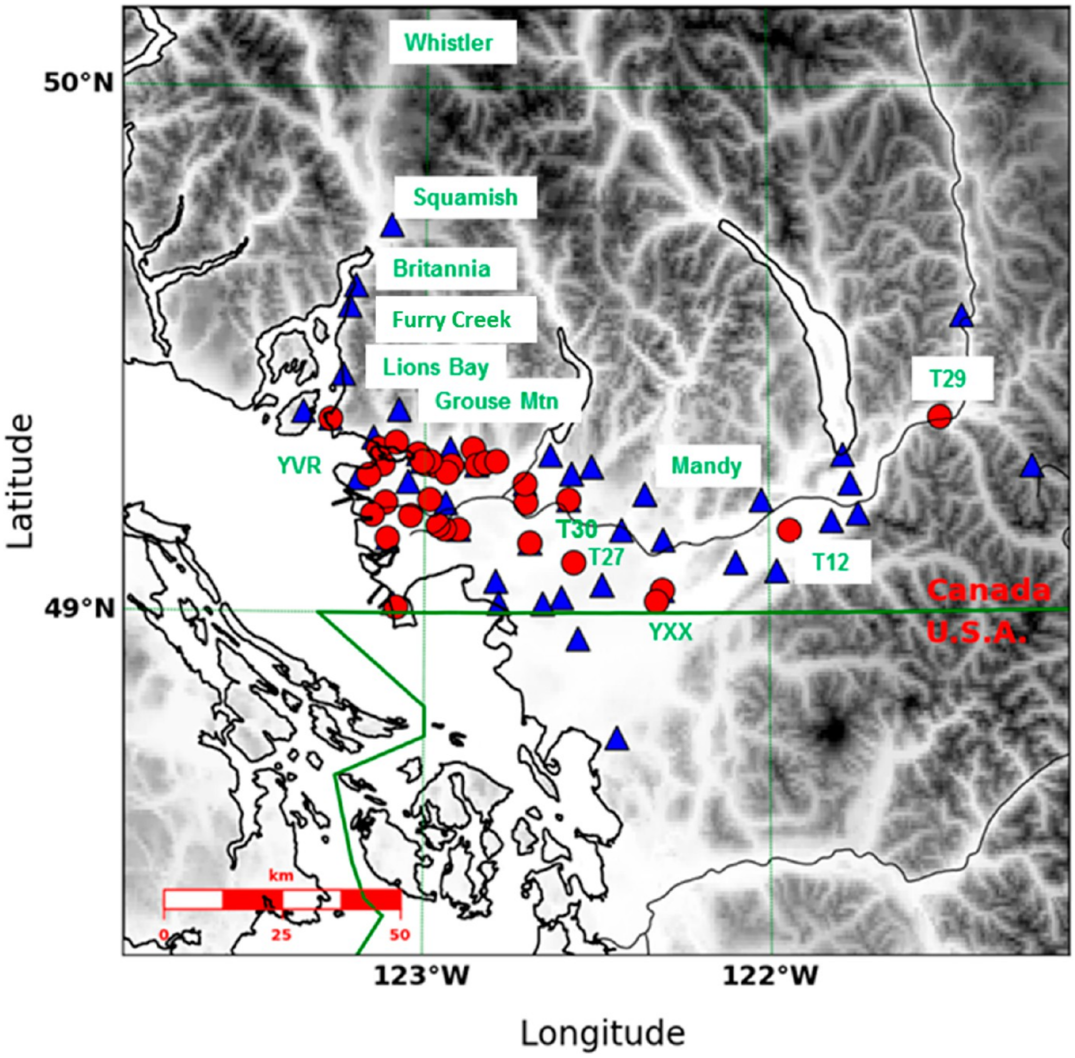

Figure 1. Map of southwestern British Columbia showing the Lower Fraser Valley network of monitors with regional and government fixed monitors (red circles), GSS monitors (blue triangles); and topographic shading (gray scale). In addition, various geographic locations have been labeled (green). For concision purposes, YVR refers to Vancouver International Airport, YXX to the Abbotsford International Airport (the location of both a MetroVancouver and GSS monitoring stations), T12 refers to the MV monitoring station in Chilliwack, T29 to the MV station in Hope, T27 to the MV station in Langley, T30 to the MV station in Maple Ridge; Mandy to the GSS station at Mandy's General Store, and Grouse Mountain to the high elevation GSS Grouse Mountain site. Finally, the GSS stations along Howe Sound (Lions Bay, Furry Creek, Britannia, and Squamish) have also been labeled, as well as the Environment Canada high-elevation monitoring station at Whistler B.C.

Pakistan[2] and Mauritius,[3] respectively. Such developments represent examples of the changing paradigm of air pollution monitoring.[4] Demonstrating that low-cost measurements have sufficient reliability is however an important issue to address.

Simple, low-cost semiconductor based instruments can provide reliable long-term measurement of atmospheric O_3, with performance that is close to that of reference analysers.[5] In field studies, GSS instruments have been shown to have performance characteristics that should enable the economical construction and operation of O_3 monitoring networks of accuracy, time resolution, and spatial density sufficient to resolve the local gradients that are characteristic of urban air pollution.[5] The present work presents a realization of that idea, using a 50 sensor test-bed in the Lower Fraser Valley of British Columbia over 3 months from May−September 2012. We describe a cost-efficient alternative to traditional O_3 monitoring that permits data collection at high spatial and temporal resolution and in locations not formally accessible with traditional methods. This novel network is deployed in the Lower Fraser Valley, where an existing and relatively dense network is maintained, where hourly O_3 concentrations may exceed 100 ppb during summer, and where the urbanized region of complex coastal terrain creates a complex environment for O_3 research. This test-bed provides a unique opportunity to rigorously evaluate this monitoring approach by permitting instrument calibration and validation against an existing high quality network. Furthermore, we demonstrate the power of this novel technology to extend and complement existing traditional fixed monitor networks in a hybrid approach. Spatial monitoring patterns are presented to demonstrate the research potential of this approach, and recommendations are made to guide future deployments of such technologies.

BACKGROUND AND METHODS

Air Quality in the Lower Fraser Valley. Air pollution meteorology of the Lower Fraser Valley (LFV) with respect to O_3 has been described previously in detail.[6] In short, the LFV is a broad triangular shaped valley bounded by the Coast Mountain range to the north, the Cascade Mountains to the Southwest and Georgia Strait to the West (Figure 1). It stretches ~90 km from east to west and straddles the 49th parallel (U.S.A./Canada border). Despite a growing population of approximately 2.4 million, a combination of mitigation strategies and technological improvements has led to a decline in photochemical smog episodes. The Canada Wide Standard for O_3 (8 h average of 65 ppb) is now rarely exceeded, and only occasional exceedances of the previous 80 ppb National Ambient Air Quality Objective (hourly) occur downwind of the main urban concentration at the western end of valley.

Routine air quality monitoring in the LFV (see www.metrovancouver.org) is conducted at 26 stations located from Horseshoe Bay in West Vancouver to Hope (Figure 1). There is a concentration of stations in the heavily populated western portion of the valley bottom while under-populated areas including tributary valleys and mountainous regions have less monitoring. The calibration procedures for these instruments (MetroVancouver: personal communication) allow a maximum deviation (rarely found) of ±15%.

Several aspects of the LFV make it suitable as a test-bed for high density monitoring using GSS sensors. In particular, it:

- has excellent cell phone coverage and a reasonably dense, reliable, and well-maintained existing network for reference and calibration purposes;
- has a rich history of scientific O_3 research: including two major field campaigns (Pacific 1993[7] and Pacific 2001[8]) and ongoing research in the areas of ozone transport by slope and valley flows;[9,10,23] the vertical distribution of ozone and hand-over processes;[11,12] the spatial distribution of ozone under summer time fair weather events;[13] and the possible impacts of climate change on local ground-level ozone concentrations;[14] and
- encompasses a variety of environments (urban to rural, forested and agricultural, mountainous, and coastal).

Instrumentation—Gas-Sensitive Semiconductor (GSS) Sensor and Installation. Technical details of GSS sensors have been previously described in detail.[5,15,16] In summary, the sensor is based on conductivity changes of heated tungstic oxide, is a low powered device (~1 W) that can be operated on solar power, and has been successfully coupled with cell phone technology to enable monitoring in remote locations. The combination of long-term stability, self-diagnosis, and simple, inexpensive repair means that the cost of operation and calibration of the instruments is significantly reduced in comparison with spectroscopic reference instrumentation. Figure 2 shows the various components of the sensor and instrument manufactured by Aeroqual Ltd., while Figure 3 (left panel) shows a typical field deployment in the Lower Fraser Valley with solar panel attached. Figure 3 (right panel) shows a typical setup at a fixed monitoring site. The instrument implements a temperature step to reset the surface and an air-flow step to modulate specifically the signal due to ozone. Two sensor resistance values are measured: the air flow over the sensor is modulated between zero and approximately 100 mL/min, the resistance measured during the low-flow phase when ozone is significantly decomposed on the warm plastic surfaces surrounding the sensor being the "zero" or "baseline" resistance measurement, R_b, and that during the high-flow phase being the "gas" measurement, R_g .The ozone concentration is derived from the measured sensor resistances using a nonlinear

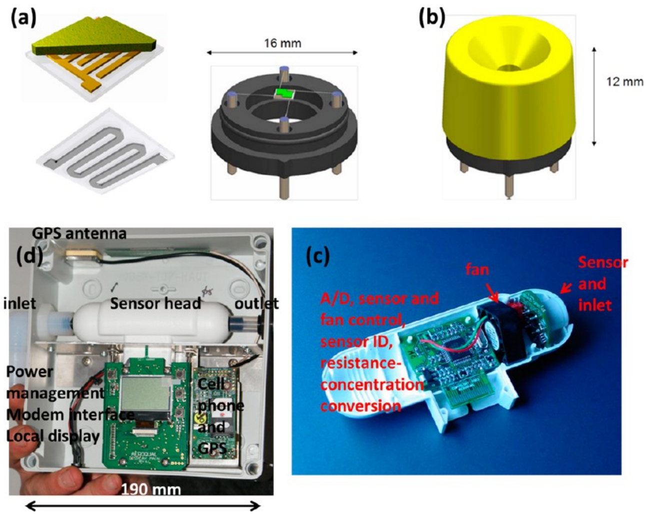

Figure 2. Sensor and instrument construction. The sensor (a) is printed on an alumina tile, 2 mm square, mounted by fine Pt wires in a housing (b) which directs onto the sensor an air flow, driven by a fan mounted on the base of the device, in the head unit (c), which holds all the sensor-specific calibration information. The rest of the instrument (d) handles data storage, presentation, and communication.

calibration loaded into the instrument.[5] Full details of the laboratory calibration are given in the Supporting Information, SI. With this method, small baseline drifts and potentially interfering signals such as that due to water vapor cancel (see SI).[16] Every minute the instrument returned the calculated ozone concentration together with the two measured resistances. The low-cost instruments were first installed adjacent to one particular reference station (Figure 3) and the calibration was verified and aligned to the Metro-Vancouver instrument before field deployment.[5] Calibration adjustment slopes and offsets were determined over at least 48hr using hourly averaged data obtained at 1 min measurement frequency. For the set of deployed instruments these were 0.9 ± 0.2 and 6 ± 6 ppb respectively with standard error of estimate over a typical range 0 − 50 ppb of 3 ± 2 ppb. These values are consistent with previous experience.[5] The nonunit slope and nonzero offset arise because the calibration parameters loaded into the instrument are derived in a factory calibration that uses a nonlinear fit of sensor resistances predicting ozone concentration, with only a small number of calibration points: see the SI. Issues with this setup were that the GSS instruments did not sample exactly the same air as the reference instrument (see Figure 3). In some cases, the range of ozone concentration observed during the field calibration was too small to give a reliable calibration across the required range and in these cases, the factory calibration was used. Both problems can be overcome if the field calibration setup allows the use of an ozone generator to periodically inject higher concentrations of ozone into the inlet, as implemented previously[15] but not possible for this temporary deployment.

With a high-density network and especially with one spread over a significant geographical area, maintenance and data validation are significant issues. Routine, regular calibration, such as is applied to the reference network, is too expensive to be practical. In other work,[17] we have explored the use of correlations across the network to generate alarms, with the network being "trained" on data obtained when the instruments

Figure 3. Left: typical station photograph as deployed in the field in the LFV. Right: typical fixed monitor (Metro Vancouver) installation (Kitsilano High School) with eight GSS sensors mounted on an adjacent rack for field calibration alignment.

are newly deployed, but this method was of only limited use in the present study because of the relatively short period of deployment. In the absence of a present complete solution to the problem of data validation without regular calibration, we have used several criteria to accept valid data from the low-cost instruments. Obvious failures, such as loss of power, broken wires, delamination of the sensor material off the sensor substrate, and blocked air intakes were easily recognized and eliminated. The data were then examined according to the following criteria. Data that passed all the criteria were accepted. In the SI, we give examples for each.

(1) The low-cost instruments derive a "zero" by modulating the air flow over the sensor from a low value ("zero" or "baseline" resistance measurement). This value should remain stable over time[5]

(2) The values observed should be constrained by general expectations of the behavior of the ozone concentration, which is in any case shown by the general behavior revealed by the reference stations. These expectations include that the ozone concentration should usually be low during the night and should show a daily variance that is reasonably consistent over time. In essence, these ideas are a different expression of the idea of a probability of any given average or variance across some time period conditional on the values observed from nearby stations. Large and highly localized variations can of course confound this expectation, but we did not note anything like this during this particular deployment

(3) We plotted the ozone concentration returned by the instrument, P_{calc}, against $(R_b - R_g)$. This nonlinear relationship should remain stable if the calibration loaded into the instrument remains valid. In essence, the sensor is being checked against a model for its response. The major reason for a change is that the high-rate air flow across the sensor might drift over time.

Modeling. As a means of evaluating the performance of the hybrid network, we compared spatial fields with spatial fields generated by the Unified Regional Air-quality Modeling System (AURAMS[18]). Briefly, this photochemical model was run over a four day period using a nested configuration of 12- and 4-km grid spacing with the inner (4-km) domain covering and extending well beyond the area serviced by both the fixed and GSS ozone monitoring networks. Meteorology for the simulations was provided by Environment Canada's Global Environmental Multiscale (GEM[19]) weather forecast model run at a 2.5-km resolution and then interpolated to the AURAMS domains. Emissions for the model were processed using the Sparse Matrix Operator Kernel Emission (SMOKE[20]) processing system using 2006 Canadian and 2005 U.S. emission databases. Emission totals for both databases were pro-rated to 2012 levels using Metro Vancouver forecasted and backcasted LFV emission estimates (GVRD[21]). Evaluation of the model against the MV network showed a network wide average Root Mean Square Error (RMSE) of 10.8 ppb and a Mean Bias Error (MBE) of −2.6 ppb.

RESULTS

Network Performance over Time. Figure 4 shows over time the number of devices in the GSS network that were

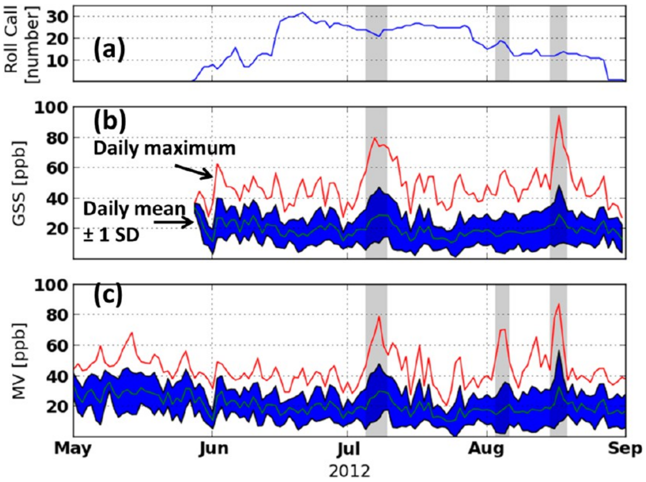

Figure 4. (a) The number of GSS stations (per day) with at least one 8-h period with continuous data. (b),(c) Daily average (±1 standard deviation) and daily maximum ozone concentration recorded by the GSS network (b) and the reference network (c). Three significant ozone episodes are highlighted.

delivering accepted data and compares the daily network averages for the GSS network with those for the reference station network. The two networks were highly correlated on average, supporting the contention that the GSS network produced reliable data. The reliability of the GSS device results and the reliability of the calibration alignment procedure were assessed by colocating devices with MV reference stations. Figure 5 shows observed hourly ozone concentrations (in ppb)

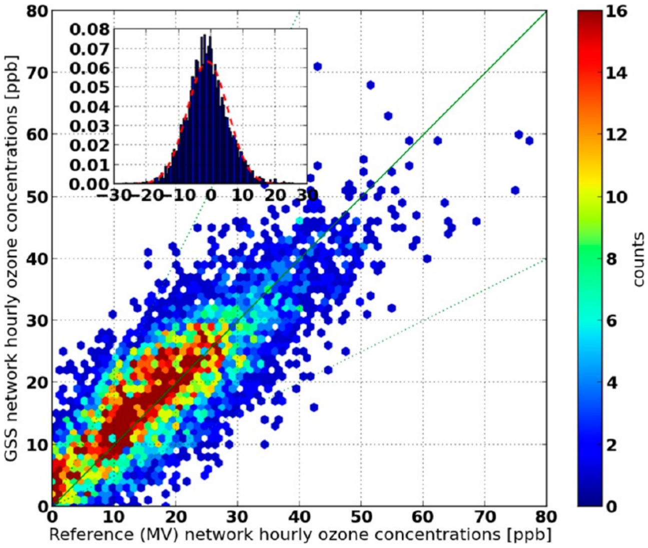

Figure 5. Hexbin plot of observed hourly ozone concentrations (in ppb) from the ten colocated MV and GSS monitors using a total of 6203 measurement pairs. The inset shows the distribution of differences, (GSS-MV), with fitted normal distribution.

with the data acceptance criteria applied, as described above, from 10 GSS instruments, each colocated at a different MV site, with a total of over 6000 data pairs. The data show standard error of estimate of 6 ppb. There is no significant bias from the line of unit slope and zero offset (mean bias −1 ppb). The errors are normally distributed, part of which will be due to the reference instruments, with very few single-point outliers. The contribution of the GSS instruments to the standard error is most likely due to measurement error in the sensor resistances. Identification of the reason for single-point outliers is difficult. Possibilities include issues with air flow into the sample inlet, very localized and temporary effects of dust in the air, and that there could be, over short time scales, rather large and very localized variations in ozone concentration, caused for example by reactions with emissions from nearby stationary motor vehicles.

At full deployment, there were approximately 30 GSS devices operating reliably, although up to 50 had been deployed (Figure 4a). The number producing reliable data then fell over about a month before stabilizing at 20−25 devices. The network was then reconfigured, with devices being removed and moved out to the periphery of the valley. There were several reasons for failures that are easily addressed. First, there was an error in the temperature setting of some of the sensors, which led to a premature failure. Second, May−June 2012 in Vancouver was exceptionally rainy: there was insufficient sunlight to charge the backup batteries on devices installed in remote locations. Third, devices installed close to the U.S. border picked up U.S. cell-phone stations and consequently incurred international roaming charges: these were necessarily disabled, although the devices did continue to operate and store 10-min averaged data on-board. Devices that were deployed in the U.S.A. implemented this feature. Fourth, maintaining stable air-flow across the sensors was a significant issue and accounted for most of the failures: the inlet pipes were narrow and easily blocked by spider webs and other insects. Finally, in some locations, dust and dirt on the inlet filters and dirt which passed through the filters and deposited on the sensor caused ozone decomposition and hence loss of signal. There was a significant drop in numbers of acceptable device results on Saturday, July 28th, the first night of the Celebration of Light Fireworks Show. After the network was dismantled, the sensors were examined: black specks were observed on the WO_3 sensor element of many of the failed devices, possibly due to smoke.

These issues can be addressed by simple changes to the instrument and operating practice. For example, it is simple to build redundancy into the devices to address issues for remote or critical sites. A "sleep" mode can be implemented to conserve battery if there is inadequate sunlight for charging, or can be combined with remote activation of the instrument so that measurement is made only over desired times rather than continuously. Power can also be conserved by transmitting data less frequently. The air inlet needs to be designed more carefully, to screen out dirt more effectively and prevent insect ingress without causing significant ozone decomposition on the filters, and the fan can be replaced by a small air pump, for more reliable flow. Finally, the data screening techniques that we used can be automated so that problems can be identified rapidly and the sensor head changed.

Temporal Patterns and Associated Meteorological Context. In Figure 4, the course of mean, maximum, and standard deviation of hourly ozone at all GSS sites (Figure 4b) and at the fixed MetroVancouver (MV) monitors (Figure 4c) for the complete deployment is shown. Of note again is the strong agreement between both time series, although some subtle differences are evident. This is consistent with expectations based on the calibration and previous deployments.[5] Two significant ozone episodes (July 7−10 and August 14−18) are highlighted in Figure 4 in which ozone concentrations approached or exceeded Metro Vancouver's 1-h ozone objective of 82 ppb. A third minor episode is evident in the MV time series (August 1−4) but not in the GSS data set, pointing to a sensitivity to the different geographical distribution of instruments in the two networks.

Both the July 7−10 and August 14−18 events were typical of the region,[22] in that they were characterized by upper-level atmospheric ridging, surface high pressure over western Canada, coupled with a weak thermal trough over the coast or southwestern U.S.A. The combination of these meteorological patterns, which occur on average half a dozen times a year, produces clear skies, high temperatures, and light winds. Depending on the relative strength and positioning of the thermal trough and continental high pressure patterns, the usual sea-breeze circulation may be suppressed, which, in such cases, leads to stagnant conditions and usually the region's worst summertime air quality. Such was the case for the August 14−18 episode, which was characterized by high temperatures (peak daytime temperatures inland of 33.3 °C (Abbotsford) and 27.6 °C at the coast (Vancouver International Airport)), low daytime winds (<2 m/s for many hours inland at Abbotsford) and cloud-free skies (see Figure 1 for station locations). The July event was not as pronounced (peak temperatures of 27.8 °C at Abbotsford and 25.0 °C along the coast) and was windier (daytime winds in excess of 4 m/s at Abbotsford). Both events terminated when the surface pressure patterns shifted, allowing a surge of clean and cool marine air to ventilate the valley.

In both events, ozone concentrations increased from day to day. For the August event, ozone concentrations peaked on the 17th, with exceedances measured by the MV network at across the valley: Maple Ridge (T30; 87 ppb), Langley (T27; 86), Abbotsford (T33; 83) and Chilliwack (T12; 84). Correspondingly high (>80 ppb) concentrations measured by the GSS network had 95 ppb at Mandy's Store (midvalley) and 87 ppb at Furry Creek (northwest of downtown Vancouver). For the July episode, peak hourly readings seen by the MV network occurred in the eastern part of the valley: Hope (T29; 79 ppb), Chilliwack (T12;74) on July 8th. Peak concentrations measured by the GSS network showed 74 ppb at the Abbotsford site on July 8th, but also showed a peak reading of 80 ppb on the 7th at Furry Creek (see Figure 1 for station locations).

It is interesting to note that the minor August 1−4 event seen in the MV data set had meteorological conditions similar (but not as pronounced) as the August 14−18 event, but this episode occurred over a summer long weekend, which would have impacted the daily emission patterns.

Finally, during the July episode, hazy skies, attributed to wildfire smoke originating in Siberia (Environment Canada, 2013 in preparation), produced exceedance ozone levels at the elevated (2182 m agl) Whistler B.C. (approximately 50 km north of the most northerly GSS Squamish site) monitoring station (>90 ppb on July 8th) as well as further north, at the B.C. Ministry of Environment stations in Quesnel (92 ppb on July 9th) and Williams Lake (84 ppb on July 8th). While this event contributed to higher $PM_{2.5}$ values and degraded visibility in the LFV, none of the GSS or MV monitors in the LFV and those GSS sensors placed in the direct line from Vancouver to Whistler (Furry Creek, Lions Bay, Britannia Mining Museum, Grouse Mountain and Squamish) produced exceedance level readings. However, the high elevation GSS Grouse Mountain site (1231 m agl) did record near-exceedance ozone levels on the 8th (73 ppb) and 9th (75 ppb). The additional information provided by the GSS monitors is extremely helpful toward understanding both spatial extent of the smoke plume impacts as well as the mechanisms by which it descends from high elevations to the surface.

Spatial Patterns. In Figure 6, spatial patterns observed in late afternoon during the first notable O_3 event (July 8th, 2012) shown in Figure 4 are compared with the modeled ozone field for late afternoon. This demonstrates the improved resolution associated with the existing network enhanced by GSS sensors, the broad general agreement between observed and independently modeled fields and also some interesting differences in detail between these two fields.

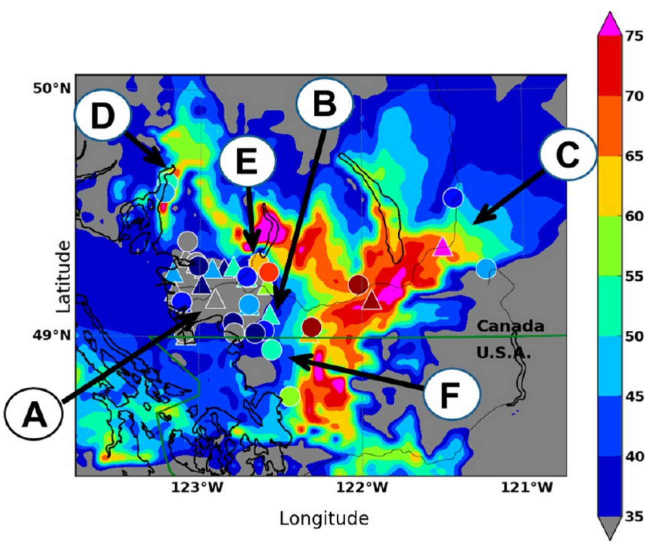

Figure 6. Modeled surface ozone concentrations for 1700 Pacific Standard Time, 8 July 2012. Observed concentrations using the same color palate are shown in filled circles (GSS) and triangles (fixed monitors). Regions and station with concentrations lower than 35 ppb (greater than 75 ppb) are shaded gray (pink). Markers A−F are described in the text.

The July 8th event shown in Figure 6 involved an unusual episode of Siberian wildfire smoke transported to British Columbia and is described above. The modeled O_3 distribution for late afternoon shows a rather complex spatial pattern with a northeast to southwest oriented swath of enhanced concentrations in excess of 60 ppb centered on the eastern portion of the LFV. A second swath extends from northwest to southeast across the northern edge of the LFV, where it merges with the higher concentrations of the eastern LFV. The model predicts low (<35 ppb) concentrations over the urbanised portions of the western LFV (likely due to titration). Observed values from both the MV and GSS instruments show broad agreement with the modeled spatial fields. Specifically, and of relevance to this study, the additional GSS sensors inserted into and beyond the existing network:

- Reveal the "well" of low concentrations in the Whiterock/South Surrey region (Label A in Figure 6);
- Capture the sharp north−south gradient separating low concentration over the main NO_x sources and higher concentration in the Eastern valley (label B in Figure 6);
- Hint at a sharp boundary in the remote eastern mountainous region suggestive of the eastern limit of the O_3 urban plume (Label C in Figure 6);
- Provide further detail along the sea-to-sky corridor extending to Whistler in the north (Label D in Figure 6) as well as concentrations along the northern mountain edge of the LFV (Label E in Figure 6); and
- Permit enhanced resolution on the south side of the U.S.A. border (Label F, Figure 6)

The GSS network emphasizes further the large spatial variability of ozone concentration within the region "A" of low predicted ozone in Figure 6, which is intensely urbanized with major roads and the port, as well as parkland. Figure 7 illustrates this variability, where instruments spaced relatively closely can show significant differences in temporal variation of ozone both during the day and during the night. Figure 7 illustrates that GSS instruments closely track the reference instruments located in the same general area, and reliably track the increase in ozone concentration inland from the urban area. The results confirm that the GSS instruments produce reliable data, revealing similar detailed spatial patterns as those revealed by the relatively high-density reference network that is deployed in this area. In the SI, we provide an animation that shows the full spatiotemporal variation of ozone across the LFV during the peak ozone day of July 8th 2012.

DISCUSSION

We report here on a novel deployment of low cost O_3 sensors within an existing monitoring network as "proof of concept" that GSS sensors enable the economical construction and operation of ozone-monitoring networks utilizing a mix of reference and low-cost instruments to deliver accuracy, time resolution, and spatial density sufficient to resolve the local gradients that are characteristic of urban air pollution. The enhanced network revealed significant smaller-scale spatial variations that were not captured either by the model or by the

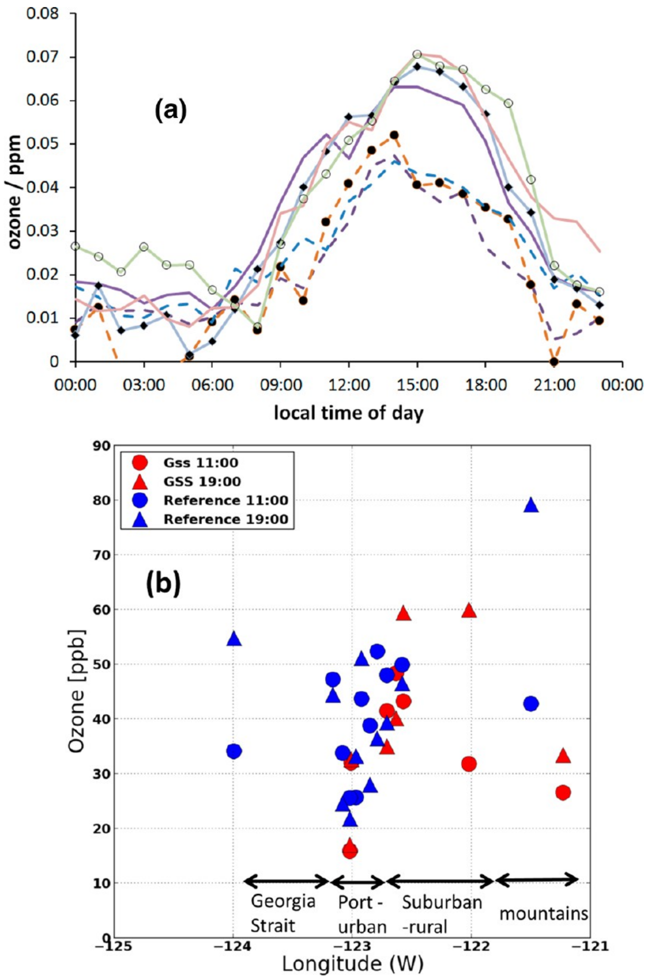

Figure 7. (a) Temporal variation of ozone concentration in region "A" (Figure 6) on July 8th 2012, comparing results from GSS instruments (highlighted with symbols) with results from reference instruments within the same general area. The curves are presented for a narrow range of latitude (49.20–49.37 °N) for the band of instruments deployed inland from the port (Figure 1). The curves marked with dashed lines are for instruments within the port zone and those with solid lines are for instruments within the suburban zone. The specific instrument locations are mapped in the SI. (b) Spatiotemporal variation along latitude (49.20–49.37 °N): ozone concentration at 11:00 and 19:00 h against longitude, comparing GSS and reference instrument results. The range of longitude for different geographical zones is approximately marked.

reference network alone. These variations were particularly evident in the intensely urbanised region A (Figure 7), where ozone would be titrated against vehicle emissions and hence where a significant spatial variability might be expected. From the technical perspective of instrument calibration and stability, this deployment demonstrated similar performance to previous studies.[5,15] Furthermore, use of a modeled field as a complement to an extensive hybrid network adds significant confidence and utility. Model predictions can be used, as here, to build confidence in the reliability of the network results. Conversely, the detail revealed by the network that cannot be captured by the model stimulates further investigation and understanding of the processes driving pollutant concentrations. The GSS sensors can be used to both increase station density within a network as well as extend monitoring into remote areas. As a result, new details can be revealed, as demonstrated by the 8 July 2012 case.

This ambitious deployment (~50 sensors) also exposed a number of challenges and lessons. The sheer logistical effort of deploying a large number of monitors at secure locations over a broad area and for a long duration should not be underestimated (this includes replacing, repairing, maintaining, and relocating instruments throughout the field study). This was perhaps the most significant challenge and clearly indicated that resources should be allocated appropriately. In addition, the summer-long study revealed deficiencies in cell phone communications and battery life (especially when poor weather compromised ability of solar panels to recharge batteries). Instrument failures at remote sites suggested that redundancy should be built into the network (especially at critical sites) as well as the possible addition of a "sleep-mode" for GSS monitors.

In this study, the selection of sites for deployment was based on a subjective analysis, and in some cases simply on the availability of secure sites. Clearly, a more objective approach to optimize interstation distances, and the "information" content of the network is preferable. This implies that more rigorous statistical approaches, and perhaps modeled fields as used above, should be utilized in the initial stages of network design.

This study has demonstrated that low-cost GSS technology embedded within a cell-based network can deliver reliable and accurate results. Potential applications include monitoring in remote areas, high density population exposure studies, the development of hybrid networks of low-cost and reference instruments that reduce overall network costs while maintaining network information, and the development of very large, spatially dense, neighborhood-scale networks ("citizen science"). Future studies will aim to further establish the network design and data processing protocols needed to build confidence in the reliability of low-cost technology, in support of the changing paradigm of air-pollution monitoring.[4]

■ ASSOCIATED CONTENT

Ⓢ Supporting Information

Descriptions of the reference station network, GSS Instrument construction, laboratory linearization of output and calibration of sensors, field calibration alignment examples, evaluation of interferences using long-term measurements at colocated stations and examples of application of acceptance criteria for data. A time-lapse video file shows the full measured spatiotemporal variation of ozone concentration across the Lower Fraser Valley on July 8th 2012. This material is available free of charge via the Internet at http://pubs.acs.org.

■ AUTHOR INFORMATION

Corresponding Author

*Phone: 604-822-4929; fax: 604-822-6150; e-mail: ian@geog.ubc.ca.

Notes

The authors declare no competing financial interest.

■ ACKNOWLEDGMENTS

We would like to thank the many individuals and facilities who generously hosted instruments as well as Adrian Jones for his work on decommissioning sites. We are also grateful to Ken Reid and the staff of MetroVancouver for the provision of data and access to sites as well as Roxanne Vingarzan of

Environment Canada for critical discussions. Funding was provided by the NZ Ministry of Business, Innovation, and Employment, Contract UOAX0709

■ REFERENCES

(1) Ramanathan, N.; Lukac, M.; Ahmed, T.; Kar, A.; Siva, P.; Honles, T.; Leong, I.; Rehman, I. H.; Schauer, J.; Ramanathan, V. A cellphone based system for large scale monitoring of black carbon. *Atmos. Environ.* **2011**, *45*, 4481−4487.

(2) Ikram, J.; Tahir, A.; Kazmi, H.; Khan, Z.; Javed, R.; Masood, U. View: Implementing low cost air quality monitoring solution for urban areas. *Environ. Syst. Res.* **2012**, *1*, 10 DOI: 10.1186/2193-2697-1-10.

(3) Khedo, K. K.; Perseedoss, R.; Mungur, A. A wireless sensor network air pollution monitoring system. *Int. J. Wireless Mobile Networks* **2010**, *2*, 31−45.

(4) Snyder, E. G.; Watkins, T.; Solomon, P.; Thoma, E.; Williams, R.; Hagler, G.; Shelow, D.; Hindin, D.; Kilaru, V.; Preuss, P. The changing paradigm of air pollution monitoring. *Environ. Sci. Technol.* **2013**, *47* (20), 11369−11377.

(5) Williams, D. E.; Henshaw, G. S.; Bart, M.; Laing, G.; Wagner, J.; Naisbitt, S.; Salmond, J. A. Validation of low-cost ozone measurement instruments suitable for use in an air-quality monitoring network. *Meas. Sci. Technol.* **2013**, *24*, 065803.

(6) Ainslie, B.; Steyn., D. G. Spatiotemporal trends in episodic ozone pollution in the Lower Fraser Valley, British Columbia, in relation to mesoscale atmospheric circulation patterns and emissions. *J. Appl. Meteor. Climatol.* **2007**, *46*, 1631−1644, DOI: 10.1175/JAM2547.1.

(7) Steyn, D. G.; Bottehnheim, J. W.; Thomson, R. B. Overview of tropospheric ozone in the Lower Fraser Valley, and the Pacific '93 field study. *Atmos. Environ.* **1997**, *31*, 2025−2035.

(8) Li, S. M. A concerted effort to understand the ambient particulate matter in the Lower Fraser Valley: The Pacific 2001 Air Quality Study. *Atmos. Environ.* **2004**, *38*, 5719−5731.

(9) Krzyzanowski, J.; McKendry, I. G.; Innes, J. L. Evidence of elevated ozone concentrations on forested slopes of the Lower Fraser Valley, British Columbia, Canada. *Water, Air Soil Pollut.* **2006**, *173*, 273−287.

(10) Reuten, C.; Steyn, D. G.; Strawbridge, K. B.; Bovis, P. Observations of the relation between upslope flows and the convective boundary layer in steep terrain. *Bound. Layer Meteorol.* **2005**, *116*, 37−61.

(11) McKendry, I. G.; Lundgren, J. Tropospheric layering of ozone in regions of urbanized complex and/or coastal terrain: A review. *Prog. Phys. Geogr.* **2000**, *24*, 329−354.

(12) Ainslie, B.; Steyn, D. G.; Reuten, C.; Jackson, P. L. A retrospective analysis of ozone formation in the Lower Fraser Valley, British Columbia, Canada. Part II: Influence of emissions reductions on ozone formation. *Atmos.-Ocean* **2013**, *51* (2), 170−186.

(13) Ainslie, B.; Reuten, C.; Steyn, D. G.; Le Nhu, D.; Zidek, J. V. Application of an entropy-based Bayesian optimization technique to the redesign of an existing air pollution monitoring network. *J. Environ. Manage.* **2009**, *90*, 2715−2729, DOI: 10.1016/j.jenvman.2009.02.01.

(14) Reuten, C.; Ainslie, B.; Steyn, D.; Jackson, P.; McKendry, I. Impact of climate change on ozone pollution in the Lower Fraser Valley, Canada. *Atmos.-Ocean* **2000**, *50*, 42−53.

(15) Williams, D. E.; Henshaw, G. S.; Wells, D. B.; Ding, G.; Wagner, J.; Wright, B. E.; Yung, Y. F.; Salmond, J. A. Development of low-cost ozone measurement instruments suitable for use in an air quality monitoring network. *Chem. New Zealand* **2009**, *73*, 27−33.

(16) Aliwell, S. R.; Halsall, J. F.; Pratt, K. F. E.; O'Sullivan, J.; Jones, R. L.; Cox, R. A.; Utembe, S. R.; Hansford, G. M.; Williams, D. E. Ozone sensors based on WO_3: A model for sensor drift and a measurement correction method. *Meas. Sci. Technol.* **2001**, *12*, 684−690.

(17) Alavi−Shoshtari, M.; Williams, D. E.; Salmond, J. A.; Kaipio, J. P. Detection of malfunctions in sensor networks. *Environmetrics* **2013**, *24*, 227−236.

(18) Gong, W.; Dastoor, A. P.; Bouchet, V. S.; Gong, S.; Makar, P. A.; Moran, M. D.; Pabla, B.; Menard, S.; Crevier, L.-P.; Cousineau, S.; Venkatesh, S. Cloud processing of gases and aerosols in a regional air quality model (AURAMS). *Atmos. Res.* **2006**, *82*, 248−275.

(19) Côté, J.; Gravel, S.; Méthot, A.; Patoine, A.; Roch, M.; Staniforth, A. The operational CMC-MRB Global Environmental Multiscale (GEM) model. Part 1: Design considerations and formulation. *Mon. Wea. Rev.* **1998**, *126*, 1373−1395.

(20) CEP. Carolina Environmental Program, Sparse Matrix Operator Kernel Emission (SMOKE) modelling system, University of North Carolina, Carolina Environmental Programs: Chapel Hill, NC; 2003http://www.smoke-model.org/index.cfm.

(21) Greater Vancouver Regional District, 2007. 2005 Lower Fraser Valley air emissions inventory & forecast and backcast. Tech. rep., GVRD Policy and Planning Department, Burnaby, BC. http://www.metrovancouver.org/services/air/emissions/Pages/default.aspx.

(22) McKendry, I. G. Synoptic circulation and summertime ground-level ozone concentrations at Vancouver, British Columbia. *J. Appl. Meteorol.* **1994**, *33*, 627−641.

(23) Seagram, A.; Steyn, D. G.; Ainslie, B. Modelled recirculation of pollutants during ozone episodes in the Lower Fraser Valley, B. C. *Air Pollution Modelling and its Application, XXII, Proceedings of 32nd International Technical Meeting on Air Pollution Modelling and its Application*, Utrecht, The Netherlands, May 7 to 11, 2012; Steyn, D. G., Builtjes, P. J. H., Timmermans, R. M. A., Eds.; Springer: Dordrecht, 2013; pp 291−294.